

Small Updates, Big Doubts: Does Parameter-Efficient Fine-tuning Enhance Hallucination Detection ?

Xu Hu^{1*} Yifan Zhang^{1*} Songtao Wei¹ Chen Zhao² Qiannan Li³
Bingzhe Li^{1†} Feng Chen^{1†}

¹The University of Texas at Dallas ²Baylor University

³The University of California, Davis

{Xu.Hu, Yifan.Zhang3}@utdallas.edu

Abstract

Parameter-efficient fine-tuning (PEFT) methods are widely used to adapt large language models (LLMs) to downstream tasks and are often assumed to improve factual correctness. However, how the parameter-efficient fine-tuning methods affect hallucination behavior remains insufficiently understood, especially on QA datasets. In this work, we systematically investigate the impact of PEFT on hallucination detection through a comprehensive empirical study across three open-weight LLM backbones and three fact-seeking QA benchmarks. For each model, we evaluate performance using seven unsupervised hallucination detection methods spanning three complementary approaches: semantic consistency based detectors, confidence based detectors, and entropy based detectors. This multifaceted evaluation enables us to characterize how PEFT reshapes uncertainty across different detection paradigms. In conclusion, our experimental results show that PEFT consistently strengthens hallucination detection ability, substantially improving AUROC across a wide range of hallucination detectors. Besides, further analyses using linear probes and representation diagnostics indicate that PEFT methods primarily reshapes how uncertainty is encoded and surfaced, comparing with injecting new factual knowledge into the models.

1 Introduction

Hallucination, the generation of fluent but fabricated or factually incorrect content, remains a central obstacle to deploying large language models (LLMs) in intensive knowledge applications (Du et al., 2024; Manakul et al., 2023; Qiu and Miikkulainen, 2024). Although often evaluated as a factual failure, hallucination is also an epistemic one: models can be confidently wrong (Tian et al., 2024;

Preprint. Under review

*Equal contribution. [†]Corresponding authors.

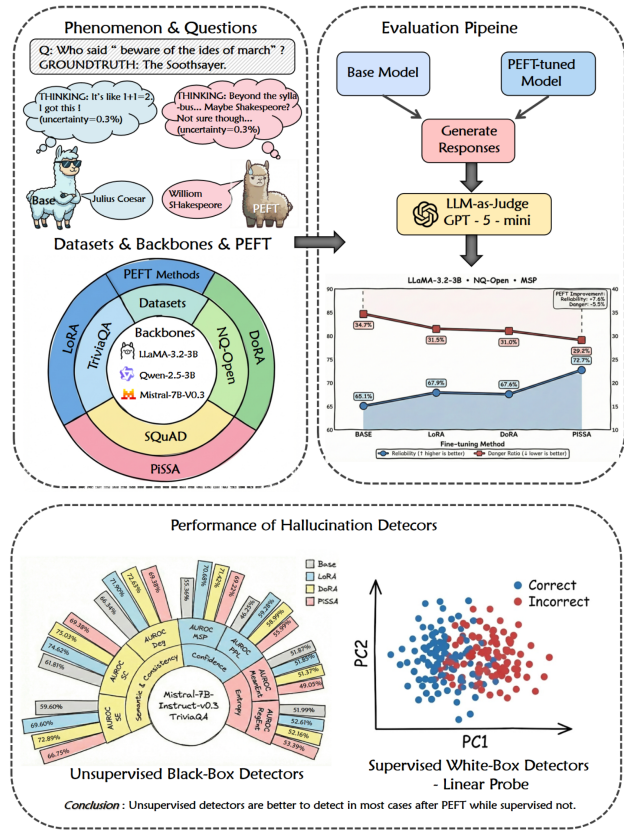


Figure 1: The overview of our empirical study of how hallucination detection ability is affected by parameter-efficient fine-tuning.

Kalai and Vempala, 2024). In practice, safety improves not only by reducing wrong answers, but by ensuring that wrong answers come with uncertainty signals that enable abstention, fallback, escalation, or filtering. Thus, systems benefit from making hallucinations both rarer and more detectable from model uncertainty (Wang et al., 2024; Li et al., 2024; Lu et al., 2024).

At the same time, LLMs are routinely adapted with parameter-efficient fine-tuning methods such as LoRA (Hu et al., 2022), DoRA (Liu et al., 2024), and PiSSA (Zhu et al., 2024). PEFT can approach full fine-tuning performance while updating only

a small fraction of parameters, and has become a de facto standard in practice. Yet PEFT is typically judged by downstream accuracy or hallucination rate, leaving its impact on hallucination detectability underexplored, even though detection pipelines rely on uncertainty and consistency based detectors, e.g. entropy, self-consistency, semantic agreement, that PEFT may alter.

Factual, open-ended QA benchmarks are a natural testbed because they combine (i) generation freedom, (ii) factual grounding, and (iii) knowledge retrieval from the model’s parameters rather than closed-set classification. Yet these settings remain relatively underexplored in PEFT studies, leaving open whether PEFT primarily (a) reduces hallucinations via improved factual competence, or (b) changes epistemic behavior by reshaping uncertainty signals used by detectors.

We address this question with a systematic study of PEFT under canonical hallucination detection settings. We compare LoRA, DoRA, and PiSSA across three open-weight backbones (LLaMA, Mistral, Qwen) and three fact-seeking QA benchmarks (TriviaQA, NQ-Open, SQuAD). Beyond QA accuracy, we evaluate a diverse suite of hallucination detectors spanning semantic consistency based, confidence based, and entropy based signals, and we also analyze hidden state changes using linear probing and PCA. Our study yields five takeaways summarized to three main conclusions:

- **Conclusion #1: Accuracy changes are modest.** PEFT yields only marginal gains in QA accuracy, implying limited direct mitigation of hallucinations through improved factual correctness.
- **Conclusion #2: Hallucinations become easier to detect.** Despite modest accuracy improvement, PEFT consistently strengthens hallucination detection signals across a broad set of black-box detectors. Our empirical observations shows the reason could be PEFT shifting scores away from the overconfident regime.
- **Conclusion #3: Supervised white-box probing hallucination detector without uniform linear separability.** PEFT induces a structured uncertainty shift in hidden representations but does not uniformly increase linear separability of correctness. Performance of white-box linear probe detection is inconsistent compared with the previous better detectability after PEFT.

Overall, these findings suggest that PEFT can act as an epistemic regularizer. It does not mainly make models know many more facts, but makes the model’s internal notion of being wrong more coherent and easier to detect from observable detectors’ signals. To our knowledge, this is the first unified study that treats PEFT as an epistemic intervention and evaluates its impact on external hallucination detectors and internal representation probes in a controlled setting.

We release code for replication of the results and further usage. Code is available at https://anonymous.4open.science/r/PEFT_for_Hallucination-CAEC/.

2 Related Work

Hallucination Detection and Uncertainty Estimation:

Fact-seeking QA is a standard test set for hallucination, with benchmarks such as SQuAD, TriviaQA, and Natural Questions (Kwiatkowski et al., 2019) providing reference answers. A major line of detection methods estimates epistemic uncertainty from *sample based* consistency and semantic agreement: SelfCheckGPT compares an answer against self-generated alternatives (Mankukul et al., 2023), while Semantic Entropy aggregates semantic dispersion among sampled answers (Farquhar et al., 2024); follow-up work proposes semantic entropy probes that map hidden representations to semantic clusters for cheaper detection (Kossen et al., 2024). Complementary logit based signals adapt maximum softmax probability and predictive entropy from out-of-distribution detection (Hendrycks and Gimpel, 2017; Farquhar et al., 2024), though calibration remains challenging in LLMs (Kadavath et al., 2022; Lin et al., 2022). Despite rapid progress on detectors, we lack systematic understanding of how fine-tuning and PEFT in particular changes the uncertainty/consistency signals these methods rely on.

Parameter-Efficient Fine-Tuning and Knowledge Dynamics:

PEFT adapts LLMs by training a small set of additional parameters while often approaching full fine-tuning performance. We study three widely used low rank methods, LoRA (Hu et al., 2022), PiSSA (Zhu et al., 2024), and DoRA (Liu et al., 2024) which share a common low rank adaptation core but differ in their parameterization: LoRA adds trainable low-rank adapters to frozen weights (Hu et al., 2022), PiSSA uses SVD based initialization from the original weights (Zhu et al., 2024), and DoRA decomposes weights into magni-

tude and direction and adapts directions separately (Liu et al., 2024). Beyond accuracy, fine-tuning can reorganize knowledge access rather than simply inject facts: narrow supervision may increase related-query hallucinations (Gekhman et al., 2024), and knowledge editing can struggle with global consistency (Zhang et al., 2024). It may also improve truthfulness while yielding mixed calibration (Tian et al., 2024), and instruction tuning can reduce blatant errors yet increase overconfidence on remaining mistakes (Perez et al., 2022). Accordingly, we evaluate PEFT through a hallucination-detection lens, focusing on its epistemic effects on detector-relevant signals.

3 Experiment

3.1 Experimental Setup

Backbones and datasets. Following the current popular hallucination detection datasets selection, we consider three open-weight instruct models: LLaMA-3.2-3B-Instruct(Grattafiori et al., 2024), Qwen2.5-3B-Instruct(Yang et al., 2025), and Mistral-7B-Instruct-v0.3(Jiang et al., 2023). For each backbone, we compare the base instruct model against its PEFT variants (LoRA, PiSSA, DoRA), fine-tuned in-domain on each dataset.

Fact-seeking benchmarks are typically presented as QA tasks with short target spans. We use TriviaQA (rc.nocontext)¹, Natural Questions (NQ-Open)², and SQuAD v1³ to probe hallucination behavior. About the data processing and selection, you can see more details in Appendix A.

Parameter-efficient fine-tuning methods. We fine-tune all models using the Hugging Face peft library. Use rank $r = 32$, scaling factor $\alpha = 64$, and dropout $p = 0.05$, AdamW with learning rate 2×10^{-5} , global batch size 64, warmup ratio 0.03, and train for 1 epoch in bfloat16. And target the attention projection layers (q_proj, k_proj, v_proj, o_proj) for all PEFT methods.

Training and evaluation loss curves for all methods and datasets are provided in Appendix G (Figures 7 and 8).

Black-box hallucination detectors. We evaluate task accuracy alongside seven hallucination detec-

tors, which fall into three groups. **Semantic consistency based methods** exploit multiple stochastic samples: Semantic Entropy (SE)(Farquhar et al., 2024) measures entropy over semantically clustered responses, SelfCheckGPT (SC)(Manakul et al., 2023) counts how many samples support the primary answer, and Degree of Uncertainty (Deg)(Lin et al., 2023) measures connectivity between sampled responses. **Confidence based methods** Maximum sequence probability score leverages the probability of the most likely sequence generation(Fadeeva et al., 2023):

$$\text{MSP}(\mathbf{y} \mid \mathbf{x}, \theta) = 1 - P(\mathbf{y} \mid \mathbf{x}, \theta).$$

Perplexity is computed as

$$P(\mathbf{y}, \mathbf{x}; \theta) = \exp \left\{ -\frac{1}{L} \log P(\mathbf{y} \mid \mathbf{x}, \theta) \right\}$$

Entropy based methods measure predictive dispersion: Predictive Entropy(Farquhar et al., 2024), also called Monte Carlo Sequence Entropy, is the negative average of log probability of response. Mean Token Entropy(Fadeeva et al., 2023) averages token entropy across the sequence.

White-box hallucination detector: linear probe. Following (Du et al., 2024; Kadavath et al., 2022; Kossen et al., 2024), we adopt the standard approach of training an external classifier for hallucination prediction using the backbone LLM’s hidden states as input. Concretely, we train logistic-regression models on a labeled training set, where labels indicate response correctness. We split the original validation set into two equal halves, which we use as a new validation set and a held-out test set, respectively. We select the hidden-state layer used as classifier input by maximizing performance on the new validation set.

Evaluation metrics. Following Yao et al. (2025), We adopt LLM-as-judge method using GPT-5-mini to label the generated response. And We report AUROC (Area Under the Receiver Operating Characteristic Curve) as the primary metric for hallucination detection. For SQuAD, we additionally emphasize AUPR (Area Under Precision-Recall Curve) due to severe class imbalance: as an extractive reading comprehension task where answers are explicitly present in the context, SQuAD yields high model accuracy (>90%) and consequently low hallucination rates (<10%). Under such imbalance, AUPR provides a more informative assessment of

¹https://huggingface.co/datasets/mandarjoshi/trivia_qa

²<https://github.com/google-research-datasets/natural-questions>

³<https://huggingface.co/datasets/rajpurkar/squad>

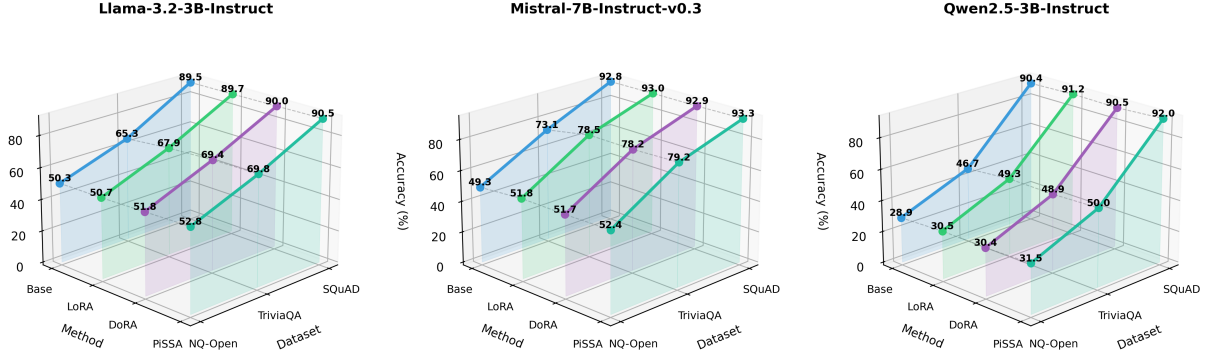


Figure 2: Test accuracy across three backbones, three datasets, and four methods. Each panel shows a 3D waterfall visualization where the x-axis shows datasets, y-axis shows methods, and z-axis shows test accuracy (%). In this paper, we define the marginal when the changes are within 1%

detection performance on the minority class (hallucinations) than AUROC (Davis and Goadrich, 2006).

3.2 Experimental Results

💡 Takeaway #1: PEFT yields modest hallucination mitigation but significant hallucination detection improvement on QA datasets. Figure 2 visualizes the test set accuracy of QA datasets across models and datasets. In NQ-Open, where base accuracy is overall low, LoRA, PiSSA, and

DoRA lift performance by only 0.4% to 3.1%, around 1.5% hallucination mitigation on average. In SQuAD, base models already approach the performance ceiling ($\approx 90\%$), and PEFT yields negligible gains of 0.1% to 1.6%. In TriviaQA, improvements range from 2.6% to 6.1%, about 3% hallucination mitigation on average. Across all configurations, PiSSA tends to outperform other methods obviously, consistent with it being the most recent advancement in PEFT.

Table 1: AUROC scores for hallucination detection baselines on LLaMA-3.2-3B-Instruct. The highest metric in each configuration is bolded. Compared to the small accuracy changes in Figure 2, the effects on these hallucination detection baselines are much more pronounced and structured. The improvement equals the best highlighted scores minus base scores. And the average improvement represents the average improvement on this dataset with the corresponding hallucination detector. The after tables follow these colour highlighting setting.

Dataset	Method	Semantic Consistency			Confidence		Entropy	
		SE	SC	Deg	MSP	Perplexity	Mean Ent.	Pre Ent.
NQ-Open	Base	0.7028	0.7432	0.7376	0.6977	0.7263	0.7295	0.6649
	DoRA	0.7453	0.7599	0.7379	0.7585	0.7445	0.7163	0.7030
	LoRA	0.7451	0.7538	0.7416	0.7620	0.7507	0.7233	0.7058
	PiSSA	0.7601	0.7806	0.7615	0.7773	0.7648	0.7381	0.7309
	▲Best Impr.	+5.73%	+3.74%	+2.39%	+7.96%	+3.85%	+0.86%	+6.60%
	▲Avg Impr.	+4.74%	+2.16%	+0.94%	+6.82%	+2.70%	-0.36%	+4.83%
TriviaQA	Base	0.8205	0.8737	0.8703	0.8154	0.8328	0.8457	0.7819
	DoRA	0.8823	0.8838	0.8738	0.8866	0.8605	0.8202	0.8138
	LoRA	0.8737	0.8889	0.8779	0.8656	0.8597	0.8303	0.8216
	PiSSA	0.8797	0.8896	0.8772	0.8878	0.8595	0.8275	0.8087
	▲Best Impr.	+5.92%	+1.59%	+0.76%	+7.24%	+2.77%	-1.54%	+3.97%
	▲Avg Impr.	+5.81%	+1.37%	+0.60%	+6.46%	+2.71%	-1.97%	+3.28%
SQuAD	Base	0.7158	0.6978	0.6764	0.6972	0.6429	0.6381	0.6808
	DoRA	0.7992	0.7715	0.6801	0.6974	0.6901	0.6923	0.6336
	LoRA	0.8027	0.7130	0.7313	0.7346	0.7074	0.7006	0.6476
	PiSSA	0.7775	0.7107	0.6855	0.6988	0.6834	0.6863	0.6107
	▲Best Impr.	+8.69%	+7.37%	+5.49%	+5.54%	+6.45%	6.25%	-3.30%
	▲Avg Impr.	+7.73%	+3.39%	+2.26%	+1.31%	+5.07%	+5.50%	-5.02%

Table 2: AUROC scores for hallucination detection baselines on Qwen2.5-3B-Instruct.

Dataset	Method	Semantic Consistency			Confidence		Entropy	
		SE	SC	Deg	MSP	Perplexity	Mean Ent.	Pre Ent.
NQ-Open	Base	0.7666	0.7761	0.7912	0.7193	0.7173	0.7225	0.6920
	DoRA	0.7780	0.8233	0.7990	0.7883	0.7264	0.6843	0.7018
	LoRA	0.7723	0.8189	0.7936	0.7817	0.7219	0.6800	0.7041
	PiSSA	0.7765	0.8178	0.7995	0.7946	0.7297	0.6874	0.7116
	▲Best Impr.	+1.14%	+5.17%	+0.83%	+7.53%	+1.24%	-3.51%	+1.96%
	▲Avg Impr.	+0.90%	+4.39%	+0.62%	+6.89%	+0.87%	-3.86%	+1.38%
TriviaQA	Base	0.8318	0.8551	0.8548	0.8132	0.8155	0.8320	0.7808
	DoRA	0.8707	0.8756	0.8642	0.8938	0.8508	0.8076	0.7899
	LoRA	0.8694	0.8796	0.8647	0.8971	0.8549	0.8145	0.7918
	PiSSA	0.8692	0.8828	0.8710	0.8973	0.8497	0.8114	0.7898
	▲Best Impr.	+3.89%	+2.77%	+1.62%	+8.41%	+3.94%	-1.75%	+1.10%
	▲Avg Impr.	+3.80%	+2.42%	+1.18%	+8.29%	+3.63%	-2.08%	+0.97%
SQuAD	Base	0.6669	0.6109	0.6599	0.6683	0.6519	0.6558	0.6314
	DoRA	0.7629	0.7412	0.7782	0.7552	0.7303	0.7313	0.6266
	LoRA	0.7533	0.7566	0.7810	0.7436	0.7295	0.7410	0.6488
	PiSSA	0.7959	0.7608	0.7728	0.7596	0.7460	0.7570	0.6246
	▲Best Impr.	+12.90%	+14.99%	+12.11%	+9.13%	+9.41%	+10.12%	+1.74%
	▲Avg Impr.	+10.38%	+14.20%	+11.74%	+8.45%	+8.34%	+8.73%	+0.19%

Table 3: AUPR scores for hallucination detection baselines in SQuAD across three backbones.

Model	Method	Semantic Consistency			Confidence		Entropy	
		SE	SC	Deg	MSP	Perplexity	Mean Ent.	Pre Ent.
LLaMA-3.2-3B-Instruct	Base	0.2456	0.2110	0.1601	0.1952	0.1849	0.1845	0.2125
	DoRA	0.2951	0.3433	0.1961	0.2219	0.2044	0.2092	0.1873
	LoRA	0.3400	0.3312	0.2773	0.3101	0.2652	0.2754	0.1751
	PiSSA	0.2640	0.2340	0.1853	0.2186	0.1951	0.2055	0.1242
	▲Best Impr.	+9.44%	+13.23%	+11.72%	+11.49%	+8.03%	+9.07%	-2.52%
	▲Avg Impr.	+5.41%	+9.18%	+5.95%	+5.50%	+3.67%	+4.55%	-5.03%
Mistral-7B-Instruct-v0.3	Base	0.1875	0.1288	0.1608	0.1736	0.1386	0.1503	0.1478
	DoRA	0.2519	0.2758	0.2773	0.2618	0.1983	0.1992	0.1195
	LoRA	0.2176	0.2294	0.2628	0.1969	0.1747	0.1898	0.1253
	PiSSA	0.2516	0.2190	0.2403	0.2121	0.1784	0.1933	0.1071
	▲Best Impr.	+6.44%	+14.70%	+11.65%	+8.82%	+5.97%	+4.89%	-2.25%
	▲Avg Impr.	+5.29%	+11.26%	+9.93%	+5.00%	+4.52%	+4.38%	-3.05%
Qwen2.5-3B-Instruct	Base	0.1787	0.1767	0.2167	0.1658	0.1534	0.1578	0.1348
	DoRA	0.3021	0.2659	0.3172	0.2572	0.2528	0.2587	0.1408
	LoRA	0.2635	0.2665	0.3330	0.2198	0.2603	0.2762	0.1549
	PiSSA	0.3113	0.2952	0.3214	0.2282	0.2622	0.2816	0.1391
	▲Best Impr.	+13.26%	+11.85%	+11.63%	+9.14%	+10.88%	+12.38%	+2.01%
	▲Avg Impr.	+11.36%	+9.92%	+10.72%	+6.93%	+10.50%	+11.44%	+1.01%

💡 **Takeaway#2: Semantic consistency based and confidence based hallucination detectors are improved significantly but entropy based detectors have marginal improvement after PEFT.**

(Tables 1, 2 and 5; see Appendix C) report AUROC scores for all hallucination detection baselines across three backbones and three QA datasets. Across all backbones and datasets, semantic consistency based and confidence based detectors consistently improve after PEFT based AUROC.

Comparing the base model and fine-tuning models across all datasets, PEFT consistently improves

semantic consistency based and confidence based methods across all the backbones and datasets. **From the average improvement of AUROC perspective**, the semantic and consistency based hallucination detectors and confidence based methods systematically raise by ranging from 0.94% (NQ-Open with degree of uncertainty) to 7.73% (SQuAD with semantic entropy) on LLaMA-3.2-3B. And for Qwen-2.5-3B, the performance has been uplifted by from 0.62% (NQ-Open with degree of uncertainty) to 14.20% (SQuAD with Self-CheckGPT). As for Mistral-7B, the scores are in-

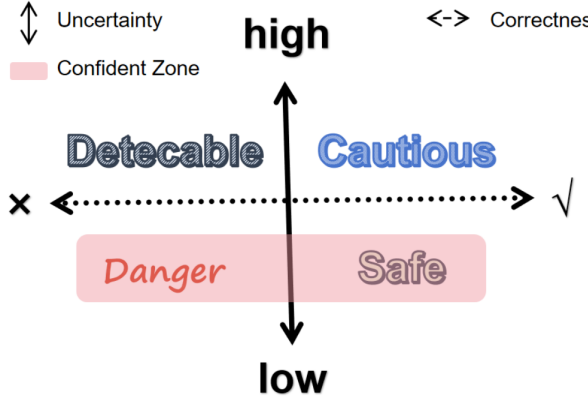


Figure 4: Uncertainty-correctness quadrant.

creased by 1.70% (NQ-Open with degree of uncertainty) to 11.18% (TriviaQA with MSP).

In contrast to semantic consistency-based and confidence-based hallucination detectors, entropy-based detectors exhibit inconsistent performance. We hypothesize that token-level entropy measures capture lexical diversity and syntactic variation, which are influenced by factors orthogonal to factual correctness, such as vocabulary choice, sentence structure, and generation randomness. In contrast, semantic consistency-based and confidence methods aggregate uncertainty at the meaning level. They align more directly with whether the model "knows" the answer. PEFT fine-tuning on QA tasks encourages the model to produce semantically coherent responses, thereby improving semantic-level calibration without necessarily re-

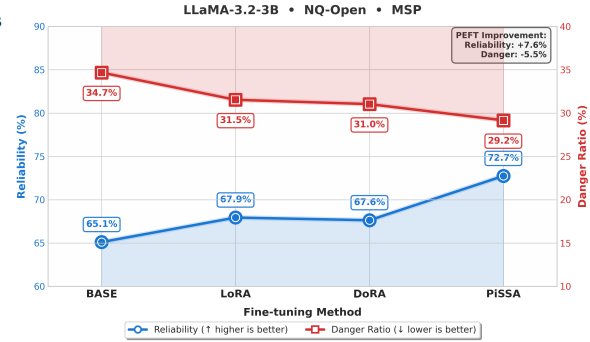


Figure 5: Uncertainty-correctness analysis on NQ-Open using MSP (Llama-3.2-3B). Reliability increases from 65.11% (Base) to 72.74% (PiSSA), indicating that responses become obviously more trustworthy after PEFT. The danger ratio also decreases by 5% (PiSSA) at most.

ducing token-level entropy.

Additionally, we report AUPR scores as a more informative metric for SQuAD in Table 3 due to severe class imbalance in SQuAD (high accuracy, low hallucination rate). PEFT also improves hallucination detection performance systematically on SQuAD across all models observed from AUPR consistent with AUROC. These results confirm that PEFT enhances hallucination detectability even under imbalanced class conditions where AUROC may be misleadingly optimistic.

💡 Takeaway# 3: PEFT improves the performance of hallucination detectors by shifting scores away from the overconfident regime. The distribution plots (Figure 3) of uncertainty

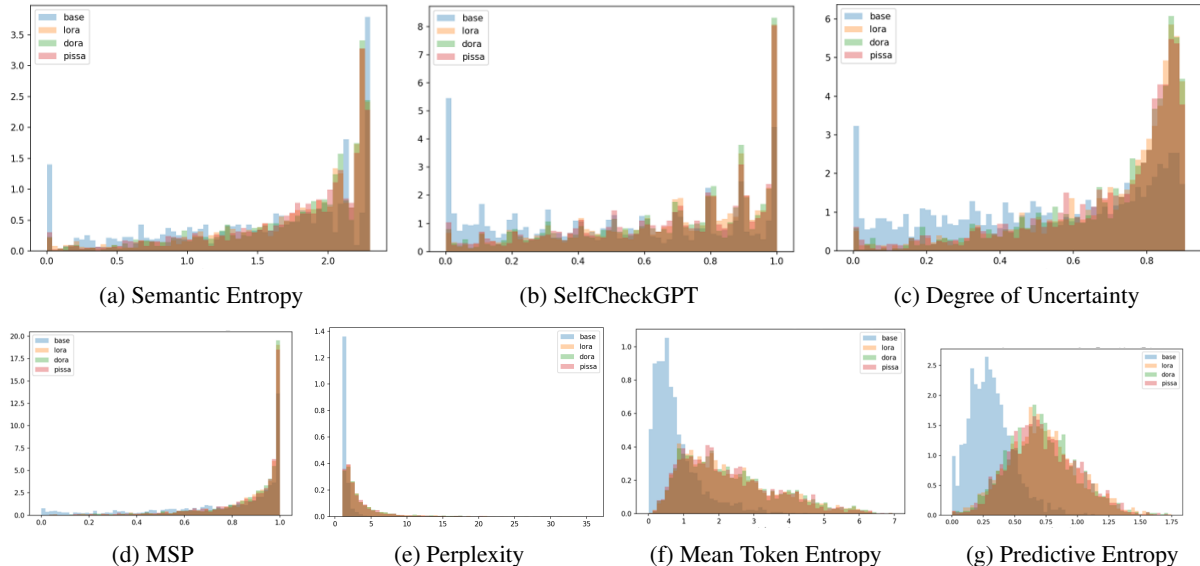


Figure 3: Uncertainty score density distributions across PEFT methods on Qwen-NQ-Open. X-axis represents the uncertainty score.

scores place heavy probability mass concentrated near the lower bound of the score range (full results in Appendix E). We further verify that such concentration reflects systematic overconfidence of hallucination detectors when applied to the base model. Specifically, we partition the model outputs into four quadrants based on uncertainty level and correctness (Figure 4). The right is the correct zone while the left is the incorrect zone. The top row is the unconfident zone while the bottom row is the confident zone. The uncertainty threshold for each model is set to its own median uncertainty score. We define the **reliability ratio** as safe / (safe + cautious) and the **danger ratio** as danger / (danger + detectable).

As shown in Figure 5, the danger ratio, which reflects overconfidence, is at a high level of 34.7%. After PEFT, it decreases consistently. (full results in Appendix F) Conversely, the reliability ratio increases after PEFT, indicating that correct outputs are more often assigned low uncertainty. Together, these shifts help explain the performance gains of hallucination detection methods under PEFT.

4 Behavior Analysis

4.1 Statistical Analysis: Track Dangerous to Detectable Migration

We track the dangerous cases of random three groups under the base model, and examine how they change after different PEFT fine-tuning methods across three datasets and two current prime and SOTA hallucination detectors (Semantic Entropy and SelfCheckGPT) on Llama-3.2-3B-Instruct. Table 4 presents the migration effects of PEFT methods. We define three metrics: **Corr. R.** (Correct / Total Danger) measures dangerous outputs corrected by PEFT; **Detect. R.** (Detectable / Total Danger) measures dangerous outputs becoming detectable; and **Conv. R.** (Detectable / (Detectable + Still Danger)) measures conversion efficiency from undetectable to detectable errors.

💡 Takeaway#4: PiSSA as the best safety protector. DoRA as the most effective knowledge corrector in open-domain QA while LoRA achieves the consistent and obvious great performance to rectify the dangers on SQuAD.

Firstly, we notice that PiSSA achieved the highest average detectable ratio. This indicates that PiSSA is particularly effective at calibrating the model’s uncertainty.

Table 4: Safety decomposition on **LLaMA-3.2-3B-Instruct**. All scores in %. The best correctness ratio and the optimal detectable ratio are highlighted in blue and pink, respectively.

Detector	Method	Corr. R.	Detect. R.	Conv. R.
NQ-Open				
SelfCheckGPT	LoRA	20.22	30.34	38.03
	PiSSA	20.97	37.08	46.92
	DoRA	21.72	34.08	43.54
Semantic Entropy	LoRA	26.25	32.56	44.14
	PiSSA	26.25	33.22	45.05
	DoRA	27.57	30.56	42.20
TriviaQA				
SelfCheckGPT	LoRA	38.64	34.09	55.56
	PiSSA	30.68	34.09	55.74
	DoRA	44.32	34.09	61.22
Semantic Entropy	LoRA	29.91	41.45	59.15
	PiSSA	29.91	45.73	65.24
	DoRA	33.33	44.44	66.67
SQuAD				
SelfCheckGPT	LoRA	45.76	37.29	68.75
	PiSSA	42.37	47.46	82.35
	DoRA	37.29	45.76	72.97
Semantic Entropy	LoRA	37.74	50.94	81.82
	PiSSA	35.85	52.83	82.35
	DoRA	35.85	45.28	70.59

Secondly, in open-domain QA datasets, including TriviaQA and NQ-open, DoRA shows the best performance to directly fix the factual errors, achieving the highest correct rate (44.3% with SCG on TriviaQA). It shows DoRA’s weight-decomposed updates may be more efficient at injecting or activating correct knowledge, and better support knowledge retrieval from parametric memory.

Conversely, LoRA dominates on SQuAD. LoRA achieves the highest correct rate (45.76%). This pattern is consistent with the observation in Figure 11. We find that on SQuAD, LoRA always reduces the danger ratio even by around 50% significantly. We guess that LoRA’s parameter-efficient updates excel at improving attention based extraction.

4.2 Case study

We show two typical cases generated from LLaMA-3.2-3B in the boxes below to illustrate the two hallucination behaviors. Their uncertainty scores are calculated by SelfCheckGPT. Additionally, the first case is from NQ-Open and the second is from SQuAD. Case 1 demonstrates how PEFT handles a factual recall question while case 2 shows an extractive QA scenario.

Case 1:

“5000 Dollar Bill” Hallucination

Q 1441: Who is pictured on the 5000 dollar bill ?
Ground Truth: James Madison

Model	Response	Uncert.	Analysis
Base	“George Washington.”	0.1024	⚠️ Dangerous
LoRA	“James Madison.”	0.6994	✅ Correct
PiSSA	“Ulysses S. Grant.”	0.9633	FLAG Detectable
DoRA	“James Madison.”	0.7893	✅ Correct

💡 **Insight:** Base model confidently answer incorrectly; PEFT models express high uncertainty. PiSSA makes the error the most detectable, while DoRA directly fixes the error.

Case 2:

“Income Inequality Increase” Hallucination

Q 220: When did income inequality begin to increase in the US? **Ground Truth:** 1970s.

Model	Response	Uncert.	Analysis
Base	“After the 1970s.”	0.0185	⚠️ Dangerous
LoRA	“the 1970s.”	0.0296	✅ Correct
PiSSA	“after the 1970s.”	0.6651	FLAG Detectable
DoRA	“after the 1970s.”	0.4810	FLAG Detectable

💡 **Insight:** Base model outputs an incorrect and confident answer with high confidence. After fine-tuning, LoRA directly corrects the prediction, while PiSSA remains incorrect but exhibits the highest uncertainty, making the error **most detectable** among PEFT variants; DoRA also stays incorrect with elevated uncertainty, but less than PiSSA.

5 White-Box Detector: An Uncertainty Probing

While the unsupervised black-box detectors (semantic consistency based and confidence based) benefit from PEFT, it remains unclear whether this improvement extends to other detection paradigms. We examine linear probing, a supervised white-box approach that directly classifies hidden representations to test whether PEFT universally enhances hallucination detectability.

💡 **Takeaway#5: PEFT raises black-box hallucination detectors but disrupts linear probe based detector.** Figure 6 reveals striking inconsistency: on TriviaQA, PEFT improves probing performance; on NQ-Open, PEFT uniformly degrades it; on SQuAD, effects vary by model. This inconsistency contrasts sharply with black-box unsupervised uncertainty detectors (Table 1, 2 and Table 3), which improve consistently almost across all settings after PEFT. The PCA visualizations in Appendix Figure 13 confirm this interpretation. After PEFT, hidden representations do not exhibit clearer separation between correct and incorrect predic-

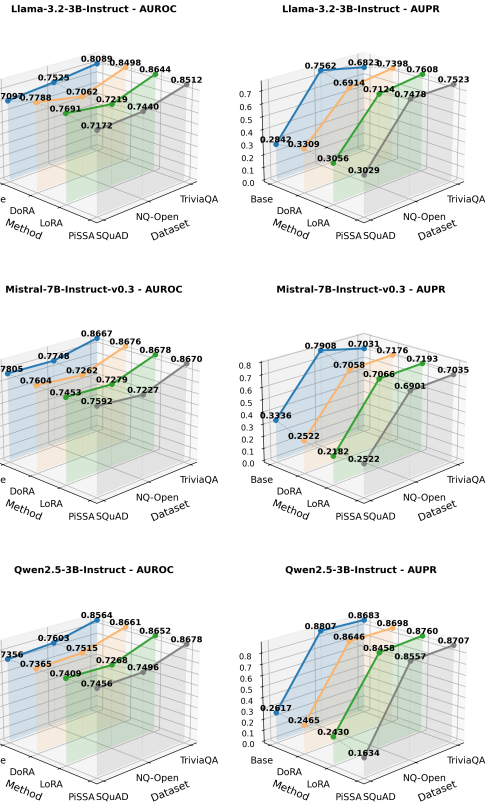


Figure 6: Probe hallucination detection scores. We train logistic regression probes on every layer’s hidden states to detect hallucination, reporting the best-performing layer’s AUROC and AUPR on the validation set. Z axis shows the AUROC/AUPR.

tions—in some cases, clusters become less distinguishable. Yet downstream detection via black-box methods improves substantially.

The divergence suggests a critical insight that supervised probing based hallucination detectors proves unreliable for PEFT-tuned models compared with the unsupervised hallucination detectors. We conjecture that PEFT redistributes uncertainty from linearly separable hidden representations to output level behaviors, disrupting the geometric structure that probes exploit. Characterizing this representational shift and developing probe methods robust to fine-tuning remains a promising direction for future work.

6 Conclusions

In this work, we present the first systematic study of how parameter-efficient fine-tuning affects hallucination detection in LLMs. Across three backbones, three PEFT methods, three QA benchmarks and eight hallucination detectors, we show that PEFT yields only marginal accuracy gains but consistently improves hallucination detectability. Our results indicate that PEFT primarily reshapes how

uncertainty is expressed, unlocking suppressed uncertainty that popular hallucination detectors can exploit. This effect is especially obvious for semantic consistency based and confidence based detectors, while token-level entropy detectors benefit inconsistently. Further analyses reveal that PEFT improves black-box uncertainty detectors but can disrupt supervised linear probe detectors. Overall, our findings position PEFT makes model’s hallucination more visible and controllable, with important implications for safe deployment and uncertainty-aware LLM systems.

Limitation

Our study has several limitations. First, we focus on three English QA benchmarks and moderately-sized models (3B–7B); generalization to other tasks, languages, modalities, or larger models remains unclear. Second, we examine only three PEFT methods with in-domain fine-tuning. Other adaptation strategies (e.g., full-parameter fine-tuning, RLHF-style training, or PEFT with explicit uncertainty objectives) may exhibit different epistemic behaviors, which we leave to future work. Finally, our analysis is restricted to fact-seeking question answering; extending this investigation to other task types—such as long-form generation, reasoning-intensive tasks, multimodal settings, and interactive dialogue, remains an important direction for future research.

References

Jesse Davis and Mark Goadrich. 2006. The relationship between precision-recall and roc curves. In *Proceedings of the 23rd International Conference on Machine Learning*, pages 233–240. ACM.

Xuefeng Du, Chaowei Xiao, and Sharon Li. 2024. Haloscope: Harnessing unlabeled llm generations for hallucination detection. *Advances in Neural Information Processing Systems*, 37:102948–102972.

Ekaterina Fadeeva, Roman Vashurin, Akim Tsvigun, Artem Vazhentsev, Sergey Petrakov, Kirill Fedyanin, Daniil Vasilev, Elizaveta Goncharova, Alexander Panchenko, Maxim Panov, and 1 others. 2023. Lm-polygraph: Uncertainty estimation for language models. *arXiv preprint arXiv:2311.07383*.

Sebastian Farquhar, Jannik Kossen, Lorenz Kühn, and Yarin Gal. 2024. Detecting hallucinations in large language models using semantic entropy. *Nature*, 630(8017):625–630.

Zorik Gekhman, Gal Yona, Roei Aharoni, Matan Eyal, Amir Feder, Roi Reichart, and Jonathan Herzig. 2024. Does fine-tuning llms on new knowledge encourage hallucinations? In *Proceedings of the 2024 Conference on Empirical Methods in Natural Language Processing*.

Aaron Grattafiori, Abhimanyu Dubey, Abhinav Jauhri, Abhinav Pandey, Abhishek Kadian, Ahmad Al-Dahle, Aiesha Letman, Akhil Mathur, Alan Schelten, Alex Vaughan, and 1 others. 2024. The llama 3 herd of models. *arXiv preprint arXiv:2407.21783*.

Dan Hendrycks and Kevin Gimpel. 2017. A baseline for detecting misclassified and out-of-distribution examples in neural networks. In *Proceedings of ICLR*.

Edward J Hu, Yelong Shen, Phillip Wallis, Zeyuan Allen-Zhu, Yuanzhi Li, Shean Wang, Lu Wang, and Weizhu Chen. 2022. LoRA: Low-rank adaptation of large language models. In *International Conference on Learning Representations*.

Albert Q. Jiang, Alexandre Sablayrolles, Arthur Mensch, Chris Bamford, Devendra Singh Chaplot, Diego de las Casas, Florian Bressand, Gianna Lengyel, Guillaume Lample, Lucile Saulnier, Lélio Renard Lavaud, Marie-Anne Lachaux, Pierre Stock, Teven Le Scao, Thibaut Lavril, Thomas Wang, Timothée Lacroix, and William El Sayed. 2023. *Mistral 7b*. *Preprint*, arXiv:2310.06825.

Saurav Kadavath, Tom Conerly, Amanda Askell, Tom Henighan, Dawn Drain, Ethan Perez, Nicholas Schiefer, Zac Hatfield-Dodds, Nova DasSarma, Eli Tran-Johnson, and 1 others. 2022. Language models (mostly) know what they know. *arXiv preprint arXiv:2207.05221*.

Adam Tauman Kalai and Santosh S. Vempala. 2024. Why do large language models hallucinate? *arXiv preprint*.

Jannik Kossen, Jiatong Han, Muhammed Razzak, Lisa Schut, Shreshth Malik, and Yarin Gal. 2024. Semantic entropy probes: Robust and cheap hallucination detection in llms. *arXiv preprint arXiv:2406.15927*.

Tom Kwiatkowski, Jennimaria Palomaki, Olivia Redfield, Michael Collins, Ankur Parikh, Chris Alberti, Danielle Epstein, Illia Polosukhin, Jacob Devlin, Kenton Lee, and 1 others. 2019. Natural questions: A benchmark for question answering research. *Transactions of the Association for Computational Linguistics*, 7:453–466.

Jiwei Li and 1 others. 2024. Factuality in large language models: A survey. *arXiv preprint*.

Stephanie Lin, Jacob Hilton, and Owain Evans. 2022. TruthfulQA: Measuring how models mimic human falsehoods. In *Proceedings of the 60th Annual Meeting of the Association for Computational Linguistics (Volume 1: Long Papers)*, pages 3214–3252.

Zhen Lin, Shubhendu Trivedi, and Jimeng Sun. 2023. Generating with confidence: Uncertainty quantification for black-box large language models. *arXiv preprint arXiv:2305.19187*.

Shih-Yang Liu, Chien-Yi Wang, Hongxu Yin, Pavlo Molchanov, Yu-Chiang Frank Wang, Kwang-Ting Cheng, and Min-Hung Chen. 2024. DoRA: Weight-decomposed low-rank adaptation. *arXiv preprint arXiv:2402.09353*.

Haolang Lu, Yilian Liu, Jingxin Xu, Guoshun Nan, Yuanlong Yu, Zhican Chen, and Kun Wang. 2024. Auditing meta-cognitive hallucinations in reasoning large language models.

Potsawee Manakul, Adian Liusie, and Mark Gales. 2023. Selfcheckgpt: Zero-resource black-box hallucination detection for generative large language models. In *Proceedings of the 2023 conference on empirical methods in natural language processing*, pages 9004–9017.

Ethan Perez, Saffron Huang, Francis Song, and 1 others. 2022. Red teaming language models with language models. In *Proceedings of the 2022 Conference on Empirical Methods in Natural Language Processing*.

Xin Qiu and Risto Miikkulainen. 2024. Semantic density: Uncertainty quantification for large language models through confidence measurement in semantic space. *Advances in neural information processing systems*, 37:134507–134533.

Katherine Tian, Eric Mitchell, Huaxiu Yao, Christopher D Manning, and Chelsea Finn. 2024. Fine-tuning language models for factuality.

Yuxia Wang, Minghan Wang, Muhammad Arslan Manzoor, Fei Liu, Georgi Nenkov Georgiev, Rocktim Jyoti Das, and Preslav Nakov. 2024. Factuality of large language models: A survey. In *Proceedings of the 2024 Conference on Empirical Methods in Natural Language Processing*, pages 19519–19529.

An Yang, Anfeng Li, Baosong Yang, Beichen Zhang, Binyuan Hui, Bo Zheng, Bowen Yu, Chang Gao, Chengen Huang, Chenxu Lv, and 1 others. 2025. Qwen3 technical report. *arXiv preprint arXiv:2505.09388*.

Zijun Yao, Yantao Liu, Yanxu Chen, Jianhui Chen, Junfeng Fang, Lei Hou, Juanzi Li, and Tat-Seng Chua. 2025. Are reasoning models more prone to hallucination? *arXiv preprint arXiv:2505.23646*.

Shaolei Zhang, Tian Yu, and Yang Feng. 2024. TruthX: Alleviating hallucinations by editing large language models in truthful space. pages 8908–8949.

Jiali Zhu, Ze-Feng He, and 1 others. 2024. PiSSA: Principal singular values and singular vectors adaptation of large language models. *arXiv preprint arXiv:2404.02948*.

A Experimental Details

- For all the implemented LLMs, we prioritize using their officially provided application programming interface (API) if available. Besides, we ignore a little bit of questions that the LLMs refuse to answer. Otherwise, we deploy the model with LLMs on $8 \times$ A6000 GPUs.
- For instruction tuning, we use a consistent prompt: "Answer the question in a short phrase.\n\nQuestion: {question}" for closed-book QA, and prepend the passage for SQuAD.
- For TriviaQA and NQ-Open, we adopt a closed-book setting and input only the question, testing retrieval from parametric memory. For SQuAD, we provide both context and question, testing grounding in provided text. Since the official test sets for TriviaQA and NQ-Open often lack public groundtruth, we adopt a split-validation strategy on the validation sets. We use 2,500 samples for training, 500 for validation, and the remaining $\sim 2,000$ (1,805 for NQ-Open) for testing.
- While the original evaluation protocol for TriviaQA is exact match score, we find it infeasible for generative language models, as the same answer may be represented with diversified texts. For one thing, For example, the question "What is the capital of the USA?" has the ground truth "Washington, D.C.". However, if the model answers "Washington" or "Washington DC", exact match may fail to recognize these as correct. For another, there are few questions that models refuse to answer which will result to a few additional effort to deal with the specific pattern to match that if using the EM/F1. In view of this, we use LLM-as-a-Judge for QA datasets. We deploy the most recently released LLM, GPT-5-mini, as our judging model and report the accuracy in percentile.

B Fine-tuning Loss Curves

(Figure 7 and 8). This section reports training and evaluation loss curves for all PEFT configurations across models and datasets. The primary purpose of these figures is to verify the correctness and stability of the fine-tuning process rather than

to compare optimization efficiency across methods. As shown in Figures 7 and 8, LoRA, DoRA, and PiSSA consistently exhibit rapid convergence, smooth loss decay, and no signs of divergence or overfitting on LLaMA, Mistral, and Qwen backbones. Training and evaluation losses closely track each other across datasets, indicating that the observed differences in hallucination detection performance in the main paper are not artifacts of unstable training, optimization failure, or misconfiguration, but reflect genuine epistemic effects induced by PEFT.

C Hallucination detection AUROC score on Mistral-7B-V0.3

(Table 5). This section complements AUROC results of hallucination detection on Mistral-7B-Instruct-v0.3.

D TriviaQA and NQ-Open hallucination detection AUPR score

(Table 6 7). This section reports AUPR scores for TriviaQA and NQ-Open, complementing the AUROC analysis in the main paper. Because open-domain QA exhibits less severe class imbalance than SQuAD, these results illustrate why PEFT-induced improvements in uncertainty detectors do not always translate into consistent AUPR gains, supporting the discussion in Takeaway#2.

E The Uncertainty Score Density

(Figure 9 and Figure 10). This section visualizes the distribution of uncertainty scores produced by different hallucination detectors before and after PEFT. These density plots provide qualitative evidence for Takeaway #3, showing how PEFT disperses degenerate near-zero uncertainty mass and restores meaningful separation between correct and incorrect responses.

F The reliability and danger ratio on Llama-3.2-3B across all datasets

(Table 11 12). This section provides a comprehensive confidence and correctness analysis across datasets using reliability and danger ratios. The figures quantify how PEFT shifts errors from confident hallucinations to detectable uncertain cases, offering behavioral evidence that PEFT improves safety-relevant properties beyond aggregate AUROC metrics.

Table 5: AUROC scores for hallucination detection baselines on Mistral-7B-Instruct-v0.3.

Dataset	Method	Semantic Consistency			Confidence		Entropy	
		SE	SC	Deg	MSP	Perplexity	Mean Ent.	Pre Ent.
NQ-Open	Base	0.7047	0.7357	0.7578	0.6791	0.6499	0.6680	0.6658
	DoRA	0.7690	0.7875	0.7730	0.7826	0.7271	0.6953	0.7123
	LoRA	0.7684	0.7922	0.7769	0.7894	0.7368	0.7058	0.7267
	PiSSA	0.7712	0.7937	0.7746	0.7850	0.7318	0.7038	0.7193
	▲Avg Impr.	+6.48%	+5.54%	+1.70%	+10.66%	+8.20%	+3.36%	+5.36%
TriviaQA	Base	0.7869	0.7966	0.8243	0.7571	0.7185	0.7396	0.7448
	DoRA	0.8891	0.9017	0.8992	0.8730	0.8229	0.7815	0.7972
	LoRA	0.8790	0.8999	0.8966	0.8694	0.8219	0.7824	0.7953
	PiSSA	0.8790	0.9008	0.8957	0.8644	0.8101	0.7703	0.8009
	▲Avg Impr.	+9.55%	+10.42%	+7.29%	+11.18%	+9.98%	+3.85%	+5.30%
SQuAD	Base	0.6833	0.6121	0.6472	0.7032	0.6547	0.6715	0.6704
	DoRA	0.7614	0.7407	0.7560	0.7350	0.7234	0.7322	0.6445
	LoRA	0.7440	0.7328	0.7638	0.7247	0.7315	0.7503	0.6611
	PiSSA	0.7596	0.6858	0.7282	0.7348	0.7275	0.7403	0.6330
	▲Avg Impr.	+7.17%	+10.77%	+10.21%	+2.83%	+7.28%	+6.94%	-2.42%

Table 6: AUPR scores for hallucination detection baselines on TriviaQA.

Model	Method	Semantic Consistency			Confidence		Entropy	
		SE	SC	Deg	MSP	Perplexity	MeanEnt	RegEnt
LLaMA-3.2 -3B-Instruct	Base	0.6750	0.7942	0.7669	0.6761	0.7245	0.7450	0.6198
	DoRA	0.7618	0.7768	0.7535	0.8011	0.7431	0.6907	0.6585
	LoRA	0.7155	0.7461	0.7030	0.7652	0.7071	0.6643	0.6198
	PiSSA	0.7782	0.8081	0.7686	0.8260	0.7826	0.7487	0.6865
Mistral-7B -Instruct-v0.3	Base	0.5960	0.6181	0.6634	0.5536	0.4625	0.5187	0.5199
	DoRA	0.7289	0.7503	0.7263	0.7142	0.5899	0.5137	0.5216
	LoRA	0.6960	0.7462	0.7190	0.7068	0.5928	0.5185	0.5261
	PiSSA	0.6675	0.7241	0.6938	0.6922	0.5599	0.4905	0.5339
Qwen2.5 -3B-Instruct	Base	0.8437	0.8668	0.8758	0.8156	0.8265	0.8488	0.8049
	DoRA	0.8544	0.8660	0.8514	0.8986	0.8530	0.8088	0.7904
	LoRA	0.8591	0.8657	0.8472	0.9016	0.8525	0.8102	0.7774
	PiSSA	0.8433	0.8633	0.8519	0.9004	0.8377	0.7992	0.7771

G Hallucination detection score

This section reports supervised linear probe results for hallucination detection using hidden states from different layers. These results support Takeaway #5 by showing that, unlike black-box uncertainty detectors, probe based methods do not consistently benefit from PEFT and may even degrade, highlighting a representational shift induced by fine-tuning.

H PCA plots of hidden state in layer

This section presents PCA visualizations of hidden representations at the best probing layers. The plots provide geometric intuition for the probe results, illustrating that PEFT does not necessarily increase

linear separability between correct and incorrect answers, even when black-box hallucination detection improves.

I Ethical Considerations

We used AI assistants (such as Claude, ChatGPT and Gemini) during the research process for: (1) polishing and editing the manuscript for clarity and grammar; (2) providing suggestions for figure design and visualization; and (3) assisting with code implementation and debugging. All AI-generated content was carefully reviewed, verified, and revised by the authors, who take full responsibility for the final manuscript.

Table 7: AUPR scores for hallucination detection baselines on NQ-Open.

Model	Method	Semantic Consistency			Confidence		Entropy	
		SE	SC	Deg	MSP	Perplexity	MeanEnt	RegEnt
LLaMA-3.2 -3B-Instruct	Base	0.6698	0.7459	0.7391	0.6758	0.7188	0.7203	0.6319
	DoRA	0.7062	0.7418	0.7070	0.7404	0.7097	0.6810	0.6558
	LoRA	0.7115	0.7412	0.7060	0.7470	0.7280	0.7003	0.6738
	PiSSA	0.7581	0.7908	0.7619	0.7803	0.7628	0.7372	0.7146
Mistral-7B -Instruct-v0.3	Base	0.6920	0.7600	0.7759	0.6742	0.6400	0.6617	0.6393
	DoRA	0.7193	0.7682	0.7515	0.7435	0.6689	0.6406	0.6810
	LoRA	0.7284	0.7716	0.7532	0.7495	0.6809	0.6522	0.6930
	PiSSA	0.7281	0.7708	0.7483	0.7394	0.6660	0.6444	0.6743
Qwen2.5 -3B-Instruct	Base	0.8769	0.8904	0.8964	0.8428	0.8532	0.8603	0.8265
	DoRA	0.8620	0.9049	0.8811	0.8770	0.8407	0.8154	0.8385
	LoRA	0.8557	0.9003	0.8771	0.8779	0.8418	0.8161	0.8391
	PiSSA	0.8538	0.8902	0.8789	0.8859	0.8385	0.8095	0.8309

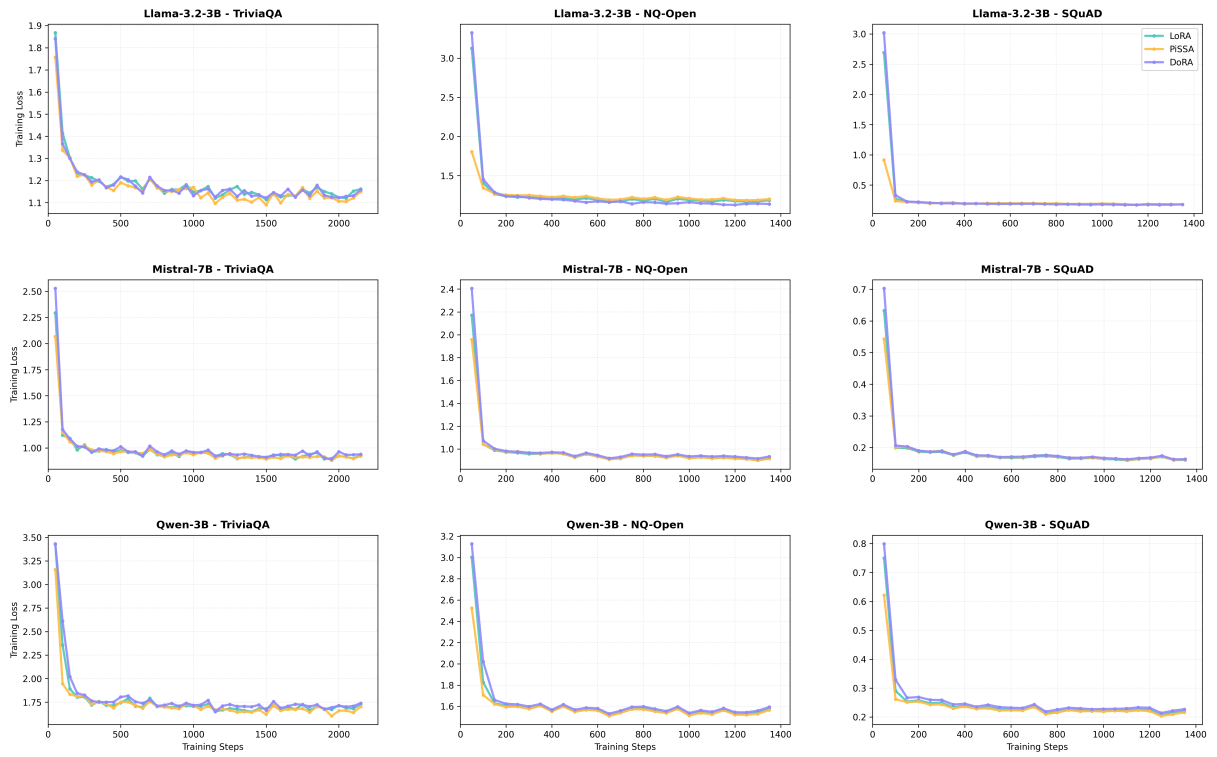


Figure 7: Training loss curves.

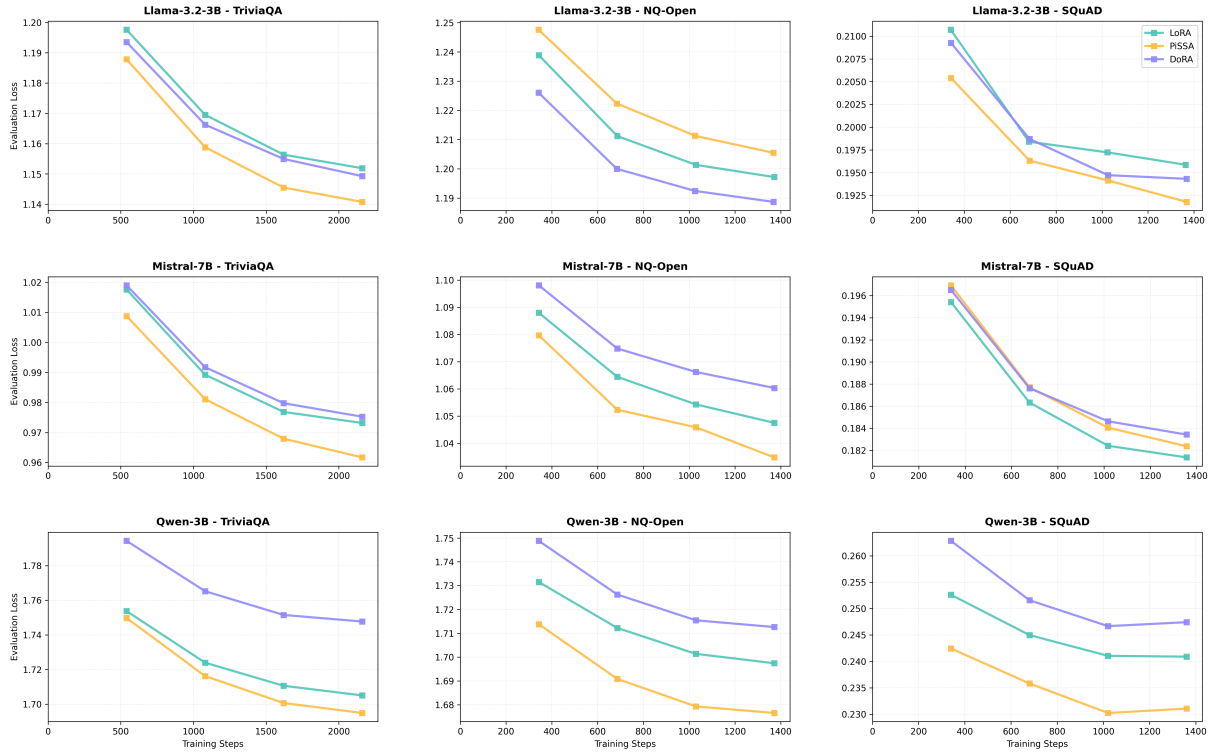


Figure 8: Evaluation loss curves.

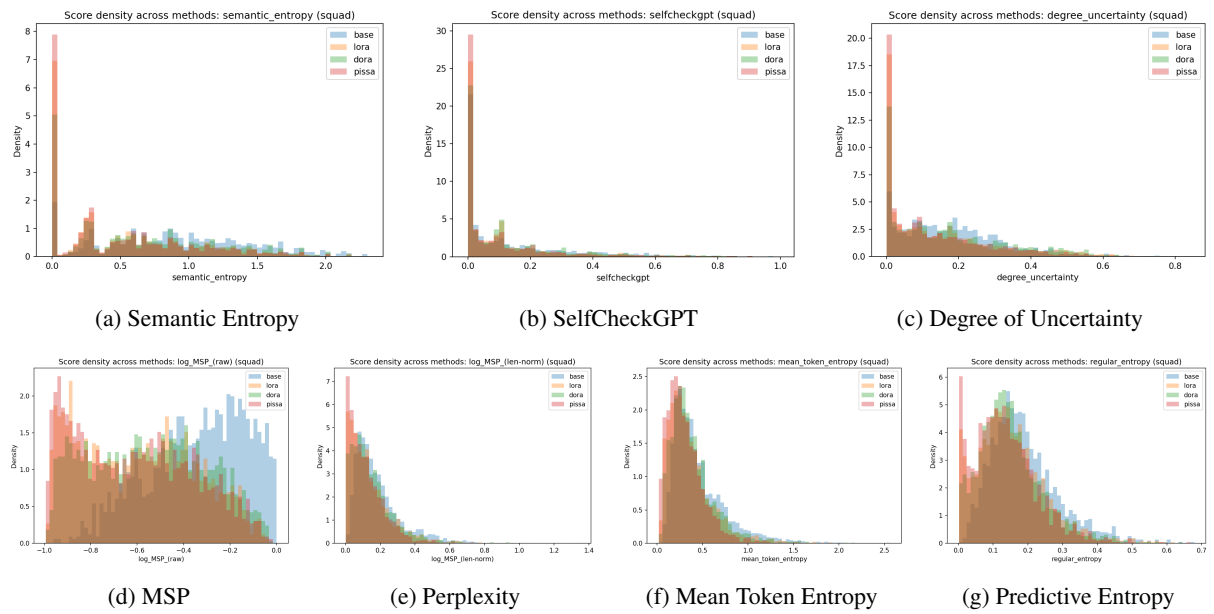


Figure 9: Uncertainty score density distributions across PEFT methods on LLaMA-3.2-3B-Instruct (SQuAD). Top row: semantic-level detectors. Bottom row: token-level detectors. X-axis represents the uncertainty score.

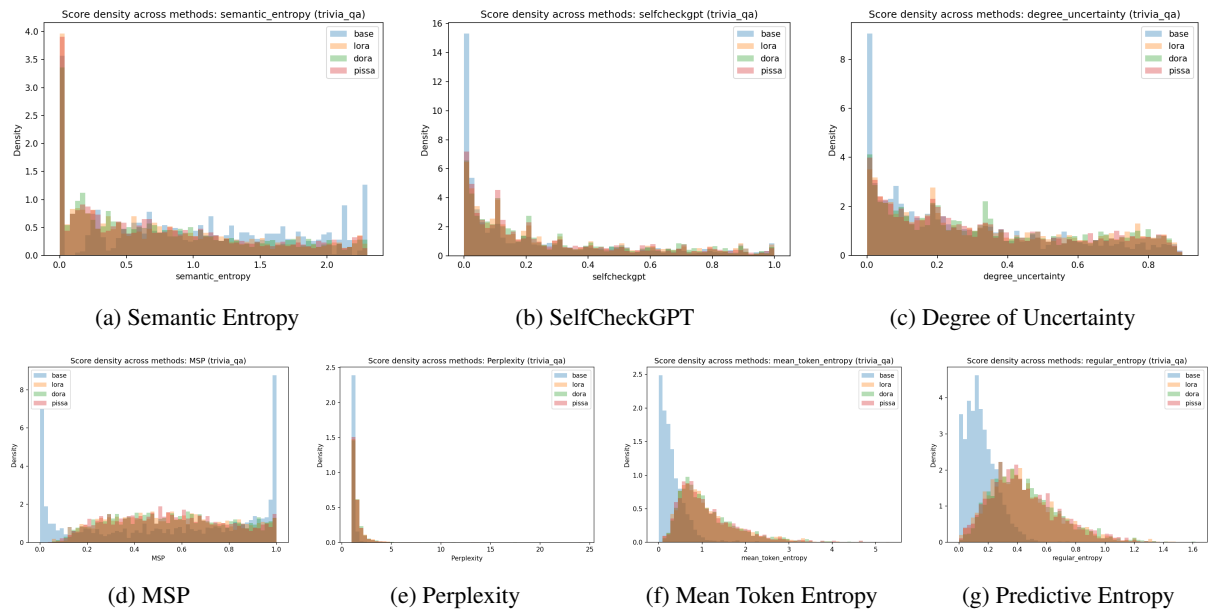


Figure 10: Uncertainty score density distributions across PEFT methods on Mistral-7B-Instruct-v0.3 (TriviaQA). Top row: semantic-level detectors. Bottom row: token-level detectors. X-axis represents the uncertainty score.

Llama-32-3B - SQuAD - Reliability vs. Danger Ratio Comparison

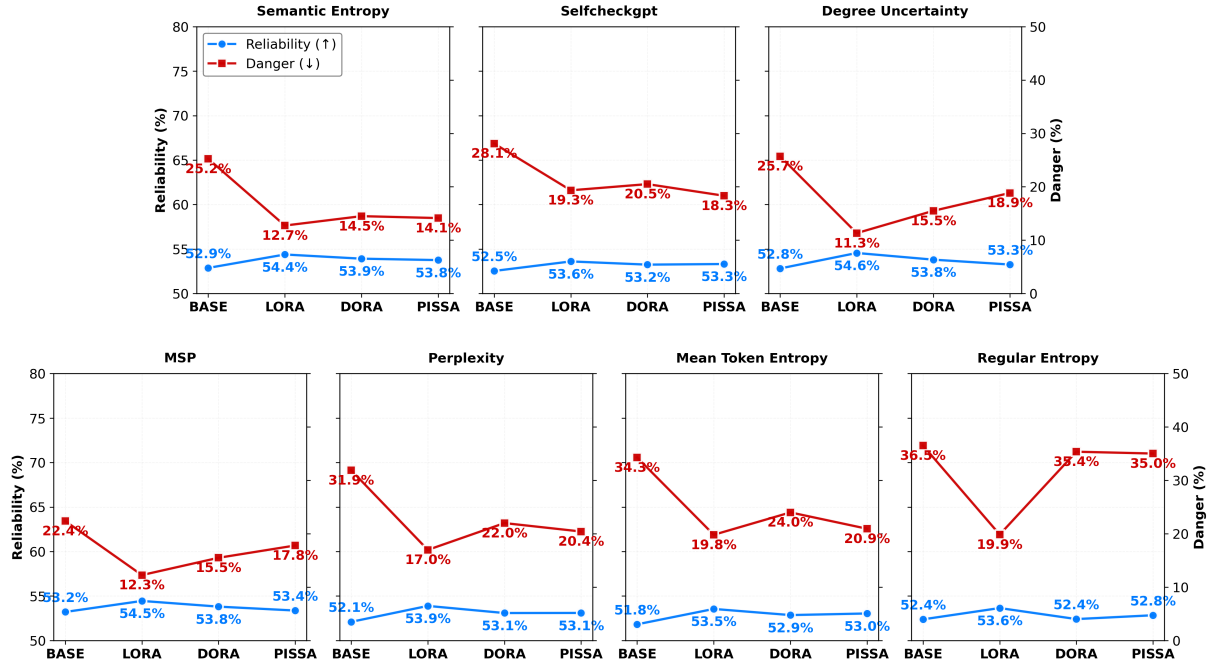


Figure 11: Confidence-correctness safety analysis on SQuAD (Llama-3.2-3B). Reliability (\uparrow): precision of high-confidence predictions. Danger (\downarrow): fraction of errors delivered with high confidence. PEFT methods reduce dangerous hallucinations while maintaining prediction reliability.

Llama-32-3B - NQ-OPEN - Reliability vs. Danger Ratio Comparison

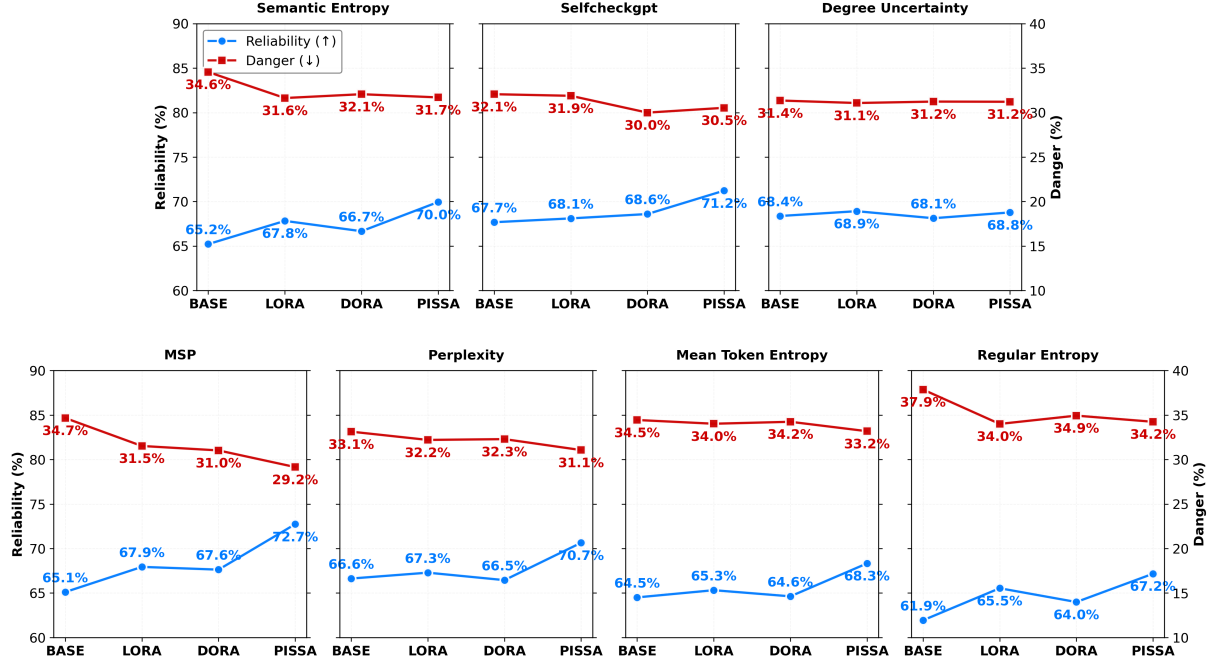


Figure 12: Confidence-correctness safety analysis on NQ-Open (Llama-3.2-3B). Reliability (\uparrow): precision of high-confidence predictions. Danger (\downarrow): fraction of errors delivered with high confidence. PEFT methods reduce dangerous hallucinations while maintaining prediction reliability.

Table 8: Layer linear probe AUROC/AUPR for hallucination detection. For each model and dataset, we train a logistic regression probe on every layer and report the best-performing layer on the test set.

Model	Dataset	Method	Best Layer	AUROC	AUPR
LLaMA-3.2-3B-Instruct	NQ-Open	Base	13	0.7525	0.7562
		DoRA	13	0.7062	0.6914
		LoRA	14	0.7219	0.7124
		PiSSA	14	0.7440	0.7478
LLaMA-3.2-3B-Instruct	SQuAD	Base	23	0.7097	0.2842
		DoRA	14	0.7788	0.3309
		LoRA	22	0.7691	0.3056
		PiSSA	22	0.7172	0.3029
LLaMA-3.2-3B-Instruct	TriviaQA	Base	18	0.8089	0.6823
		DoRA	12	0.8498	0.7398
		LoRA	16	0.8644	0.7608
		PiSSA	12	0.8512	0.7523
Mistral-7B-Instruct-v0.3	NQ-Open	Base	15	0.7748	0.7908
		DoRA	14	0.7262	0.7058
		LoRA	15	0.7279	0.7066
		PiSSA	15	0.7227	0.6901
Mistral-7B-Instruct-v0.3	SQuAD	Base	13	0.7805	0.3336
		DoRA	22	0.7604	0.2522
		LoRA	19	0.7453	0.2182
		PiSSA	18	0.7592	0.2522
Mistral-7B-Instruct-v0.3	TriviaQA	Base	14	0.8667	0.7031
		DoRA	16	0.8676	0.7176
		LoRA	16	0.8678	0.7193
		PiSSA	16	0.8670	0.7035
Qwen2.5-3B-Instruct	NQ-Open	Base	24	0.7603	0.8807
		DoRA	24	0.7515	0.8646
		LoRA	24	0.7268	0.8458
		PiSSA	24	0.7496	0.8557
Qwen2.5-3B-Instruct	SQuAD	Base	26	0.7356	0.2617
		DoRA	24	0.7365	0.2465
		LoRA	24	0.7409	0.2430
		PiSSA	34	0.7456	0.2434
Qwen2.5-3B-Instruct	TriviaQA	Base	27	0.8564	0.8683
		DoRA	24	0.8661	0.8698
		LoRA	26	0.8652	0.8760
		PiSSA	27	0.8678	0.8707

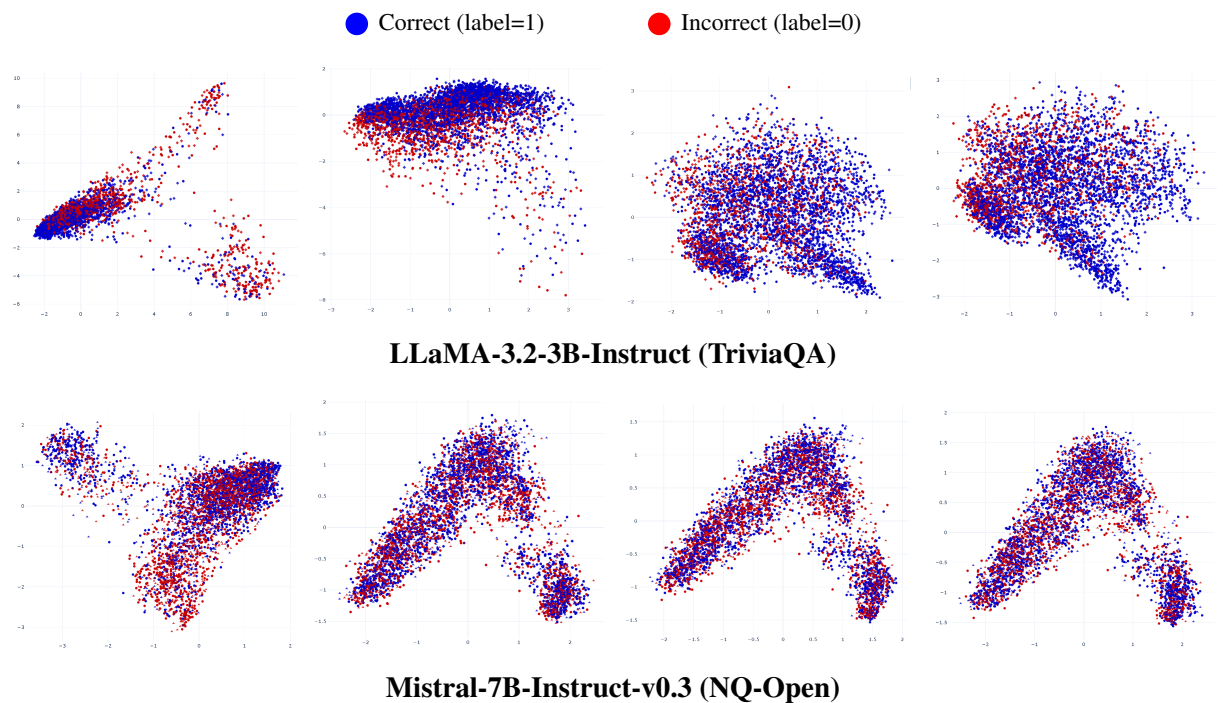


Figure 13: PCA visualization of hidden representations at the best probing layer. Each row shows Base, LoRA, DoRA, and PiSSA (left to right). It is obvious that PEFT methods almost do not separate the labels clearly.